Journal of Fluorescence, Vol. 12, No. 2, June 2002 (© 2002)

Wavelength-Resolved 3-Dimensional Fluorescence Lifetime Imaging

S. E. D. Webb,[1,5] S. Lévêque-Fort,[1] D. S. Elson,[1] J. Siegel,[1] T. Watson,[2] M. J. Lever,[3] M. Booth,[4] R. Juškaitis,[4] M. A. A. Neil,[4] L. O. Sucharov,[4] T. Wilson,[4] and P. M. W. French[1]

October 15, 2001

We have developed a compact system for wide-field fluorescence imaging, resolved in three spatial dimensions, lifetime and wavelength, that is based on a gated optical intensifier and an all-solid-state diode pumped Cr:LiSAF oscillator-amplifier system. Exploiting spectral separation, the system has been applied to human teeth, obtaining good lifetime contrast between enamel, dentin and caries. Exploiting spectral separation combined with depth resolution, the study of fluorescent microspheres led to an enhancement in both lifetime contrast and lateral resolution.

KEY WORDS: Fluorescence lifetime imaging; wavelength-resolved imaging; 3-dimensional imaging, teeth, caries.

INTRODUCTION

Fluorescence imaging most commonly uses intensity and spectral differences as the source of contrast. Such images can provide a wealth of functional information because they are dependent on the local environment of the fluorophore, as well as the chemical species itself. Spectral information from single points can easily be acquired using a monochromator, but wide-field wavelength resolution requires the acquisition of separate images with different filters in the path of the emitted fluorescence. We employ a commercially available arrangement of dichroic mirrors and filters in order to simultaneously image different spectral bands from the same field of view.

The fluorescence lifetime is an additional parameter that characterizes the fluorescence and provides complementary information to the spectral and intensity information. Increasingly, the fluorescence lifetime can be calculated for an image, rather than for a single point. Fluorescence lifetime imaging (FLIM) is a powerful tool for functional imaging that is sensitive to individual fluorophores, as well as local fluorophore environment (e.g., viscosity, oxygen, $[Ca^{2+}]$, pH etc.) [1]. For FLIM, it is preferable to resolve the measured fluorescence signal in all three spatial dimensions in order to remove the out-of-focus light that can lead to a reduction in signal contrast and incorrect lifetime values. This is typically implemented in a confocal laser scanning microscope, but to enhance image acquisition rates, other approaches have been developed. One uses wide-field illumination and a Nipkow disc to acquire data through multiple pinholes in parallel [2], which carries the disadvantage of reduced light efficiency. A second is our light efficient wide-field 3-dimensional approach based on structured illumination

[1] Photonics Group, Department of Physics, Imperial College of Science, Technology and Medicine, Prince Consort Road, London, SW7 2BW, United Kingdom.
[2] Department of Conservative Dentistry, Guys, Kings and St. Thomas' Dental Institute, London, SE1 9RT, United Kingdom.
[3] Department of Bioengineering, Imperial College of Science, Technology and Medicine, Exhibition Road, London, SW7 2BX, United Kingdom.
[4] Department of Engineering Science, University of Oxford, Parks Road, Oxford, OX1 3PJ, United Kingdom.
[5] To whom correspondence should be addressed. Tel: +44 20 7594 7745. Fax: +44 20 7594 7782. E-mail: stephen.webb@ic.ac.uk

1053-0509/02/0600-0279/0

to achieve optical sectioning without the need for pixel-by-pixel scanning [3]. To maximize the information rate, it is preferable to acquire both spectral and lifetime information from an optical section in parallel, rather than to scan pixel by pixel at various emission wavelengths. We report 5-dimensional wide-field fluorescence imaging, resolved in three spatial dimensions, lifetime and wavelength, that is based on a gated optical intensifier and an all-solid-state diode pumped Cr:LiSAF oscillator-amplifier system. In this paper, we have used the system to perform wavelength-resolved FLIM of human teeth *ex vivo* and 5-dimensional fluorescence imaging of fluorescent microspheres.

FLUORESCENCE LIFETIME IMAGING MICROSCOPE

The time-domain FLIM microscope is shown in Fig. 1 and is as detailed elsewhere [4]. Fluorescent samples were excited by ultrashort laser pulses, at 430 nm, produced by a home-built Cr:LiSAF oscillator-amplifier system. Wide-field sampling of the fluorescence decay occurs at different delays after excitation using a commercially available gated optical intensifier (GOI, Kentech Instruments Ltd., Didcot, UK). The gate width of the GOI can be set in the range <100 ps to 3 ns, and the gate may be shifted temporally relative to the excitation pulse in steps of 25 ps, over a range of 20 ns. The output of the GOI is relayed to an intensified video rate CCD camera. Typically, 20 images are averaged at each time gate. A least-squares exponential fit is performed for each pixel in the field of view in order to generate a FLIM map. For the fitting model, we commonly use a single exponential model because the calculation time is minimized. However, we have recently applied a stretched exponential function, which describes decay profiles using a continuous lifetime distribution in the sample, and thus avoids an arbitrary choice of the number of exponential terms to represent complex fluorescence decays. The stretched exponential model has produced images with an improved image quality and reduced the difference between the raw data and fitted decay curve [5]. Nonetheless, a single exponential model has been found sufficient to describe the data presented in this paper. The maximum measurable lifetime is dependent only on the repetition rate (5 kHz in this case) of the laser system; the minimum lifetime difference that may be imaged is less than 10 ps. Thus, this FLIM system exhibits excellent temporal resolution and lifetime dynamic range. By further applying the technique of optical sectioning using structured light illumination to this

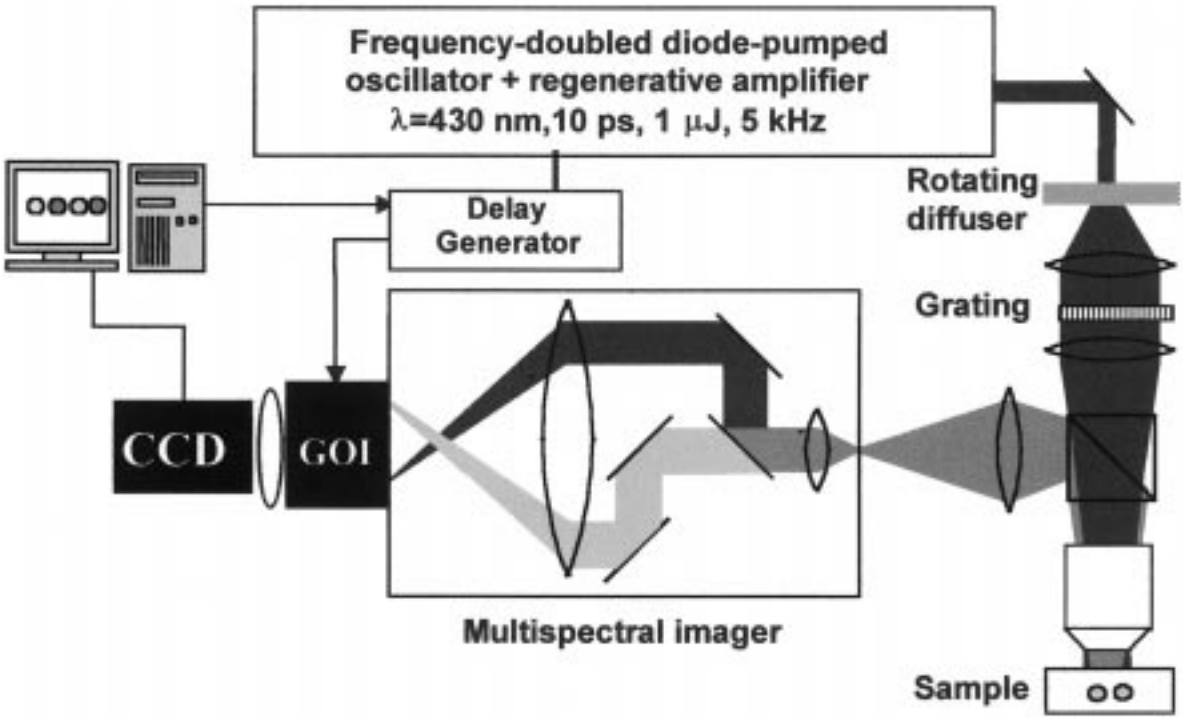

Fig. 1. Setup for wavelength-resolved fluorescence lifetime imaging with optical sectioning by structured illumination.

FLIM system, enhanced image resolution, and a greater accuracy in lifetime determination can be achieved.

The method employed here of optical sectioning by structured illumination has been described elsewhere [3]. Its implementation requires a laterally scanning grating placed in the excitation path in order to produce a modulated excitation profile at the sample. Only the fluorescence emission of the sample plane where the grating is in focus will be seen in the sectioned image. Three images I_1, I_2 and I_3 are acquired for each time gate at lateral grating positions corresponding to spatial phases 0, $2\pi/3$ and $4\pi/3$. The sectioned and conventional images, I_s and I_c respectively, are then calculated using Eqs. (1) and (2).

$$I_s = (3/\sqrt{2})\,[(I_1 - I_2)^2 + (I_1 - I_3)^2 + (I_2 - I_3)^2]^{1/2} \quad (1)$$

$$I_c = \frac{(I_1 + I_2 + I_3)}{3} \quad (2)$$

The sectioning strength of the FLIM microscope with a $\times 60$ objective (numerical aperture 0.8, normalized spatial modulation frequency 0.22) has been measured as 3 μm.

A multispectral imager [6] (Optical Insights, Inc., Santa Fe, New Mexico) placed in the emission path splits the fluorescence spectrally into two bands using a dichroic beamsplitter, in our setup at 505 nm. The device is placed in the primary image plane of the microscope and the fluorescence split such that two images are formed adjacent to one another, in the secondary image plane, on the GOI. In this way, spatially identical images differing only in their spectral content may be acquired simultaneously. The spectral content of each band and their intensities may be regulated by inserting color or neutral density filters into the path of the fluorescence. Rejecting the out-of-focus light and applying spectral discrimination improves both the accuracy of the fluorescence lifetime calculated and the fluorophore contrast.

RESULTS AND DISCUSSION

Fluorescence has been widely used in dental research, in particular to enhance our understanding of caries [7]. König *et al*. have reported that carious teeth exhibit strong red fluorescence upon 407 nm excitation, which can be explained by spectral analysis as being due to porphyrins [8]. The same authors exploited the fact that porphyrins show a very long lifetime component (10–20 ns) in addition to short decay components; these latter are due to porphyrin aggregates. They detected the presence of caries by simply acquiring a single time-gated image at long time delays after excitation, when other fluorescent components had decayed away. The drawbacks of this method are the intrinsic low light efficiency (low signal-to-noise ratio) and the information lost regarding the other fluorescent components. Our approach also uses the combination of spectral and lifetime differences of porphyrins compared to other endogenous fluorophores such as flavins and NADH; however, the excellent time resolution of our system allows the detection of the short decay components. We do not detect the long lifetime component for two reasons. Firstly, the detector gain is set appropriate to the intensity in the first time-gate after excitation and so, at long delays after excitation, when the long lifetime component dominates, the intensity is comparable to the noise. Secondly, the maximum delay range available is 20 ns, and hence the long lifetime decay components cannot be efficiently sampled. Figure 2 shows results of spectrally-resolved FLIM of teeth. Thirty video-rate images (576×576 pixels) were acquired and averaged at each of 24 different delays, from 300 ps to 11.7 ns, after excitation; data acquisition and processing took less than 5 min. The power density used was of the order of 0.5 mW cm^{-2}. The tooth used had a carious lesion present and had been extracted approximately 1 year previously and stored in an ethanol/water mixture. The tooth had been cut in half and the inner surface polished. The left half-image in Fig. 2 (a, b) corresponds to fluorescence below 505 nm; a red additive filter placed in the right channel transmitted fluorescence above 585 nm. Fig. 2(a) shows a time-gated image acquired 300 ps after the fluorescence peak, which shows contrast between the enamel and dentin in both wavelength regions. However, the carious region is not readily distinguishable. Fig. 2(b) shows the corresponding FLIM map, from which we also see good contrast between enamel and dentin in the blue channel (left half-image). The carious part of the tooth has a shorter lifetime than the healthy dentin; however, the demarcation of the carious region is blurred because of out-of-focus light. By spectral selection of the red channel (right half-image), the porphyrin emission is dominant in the right half-image. As a consequence, there is less out-of-focus fluorescence from other chemical species and the caries is better delineated. We attribute the fluorescence below 505 nm, when excited at 430 nm, to inorganic components [9].

Figure 3 shows spectrally resolved, optically sectioned FLIM maps of 15 μm and 4.5 μm fluorescent microspheres. The emission spectrum of the larger microspheres falls largely below 505 nm, the wavelength at which the dichroic beamsplitter in the multispectral imager divides the fluorescence. These microspheres are

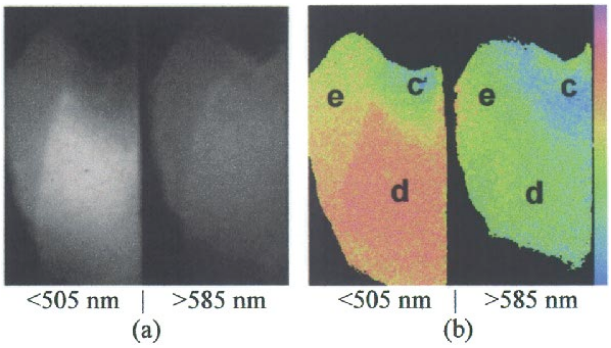

Fig. 2. Wavelength-resolved fluorescence lifetime imaging (without optical sectioning) of cut human tooth exhibiting caries: (a) time-gated intensity image. (b) FLIM map showing dentin (d), enamel (e), and caries (c), lifetime scale is 1400 (blue)—2600 ps. Thirty video-rate images (576 × 576 pixels) were acquired and averaged at each of 24 different delays, from 300 ps to 11.7 ns, after excitation.

therefore seen brightly in the left half-images of Figs. 3(a, b, c), but also weakly in the right half-images of the same figures. The small microspheres fluoresce above 505 nm and therefore appear only in the right half-image; the short-wavelength tail of their spectrum is too weak for them to appear in the left half-image. It will be observed that there are additional microspheres of an intermediate size (~10 μm diameter) present in the right half-images. We show below that these microspheres are rogue beads with the same fluorescence coating as the small microspheres.

The modulated fluorescence intensity image [Fig. 3(a)] is one of the three images at different lateral grating positions from which the sectioned and conventional images are calculated. These three images are averaged to produce the conventional intensity image [Fig. 3(b)]. Microspheres in focus are the most strongly modulated and therefore appear in the sectioned intensity image [Fig. 3(c)]. Note the residual modulation of the large microsphere toward the center of the left half-image of Fig. 3(c). Factors that contribute to this are discussed elsewhere, [10], but include imperfect grating translation and an unequal mark-to-space ratio of the grating.

One advantage of spectrally separating the microspheres is that it allows us to increase the signal dynamic range. The intensity of the large microsphere fluorescence is much greater than that of the small microspheres for 430-nm excitation. By placing a neutral density filter in the left spectral channel and increasing the GOI gain (for both channels), it was possible to level the intensity differences between the channels [see Fig. 3(a)]. Figure 3(d) shows the conventional FLIM map. The lifetimes shown for the large microspheres are different for the two channels, indicating an artefact. In the left half-image, there is a fluorescence contribution solely from the large microspheres themselves, but in the right half-image, there is an additional out-of-focus contribution from the small microspheres. Because the fluorescence lifetime is calculated from all the fluorescence contributions within the point spread function of the optical system, a single exponential fitting model will generate an average lifetime of the two contributions. By means of optical sectioning by structured illumination, we have removed the out-of-focus fluorescence. The resultant FLIM map [see Fig. 3(e)] shows the same lifetime for the large microspheres in both spectral channels because the point spread function is very narrow compared to the conventional

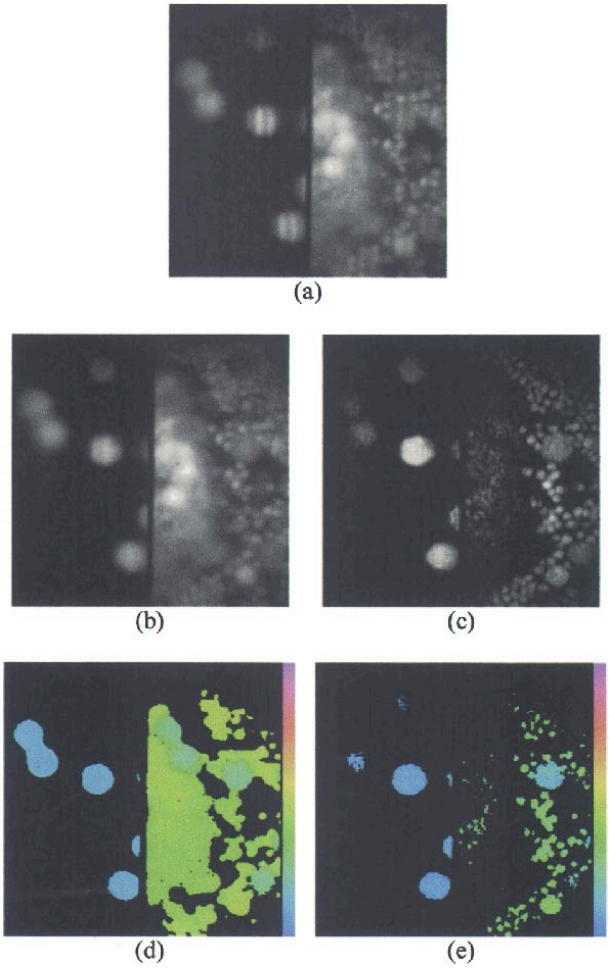

Fig. 3. Optically sectioned fluorescence lifetime imaging with spectral separation of 4.5, 10, and 15 μm diameter fluorescent microspheres; (a) time-gated modulated intensity image, (b) time-gated conventional intensity image, (c) time-gated sectioned intensity image, (d) conventional FLIM map, (e) sectioned FLIM map. Each image shows fluorescence emission <505 nm in the left half-image and >505 nm in the right half-image. Both FLIM maps have lifetime scales of 2 ns (blue) to 9 ns.

image and hence does not contain fluorescence from the small microspheres. As noted earlier, the sectioned intensity image reveals the presence of a third size of microsphere in our sample. The sectioned FLIM map clearly shows that they have the same lifetime as the small microspheres, confirming that they are rogue microspheres with the same fluorescence coating as the small microspheres.

CONCLUSIONS

A compact system for wide-field fluorescence imaging has been developed that is based on a gated optical intensifier and an all-solid-state diode pumped Cr:LiSAF oscillator-amplifier system. The system is capable of resolving *simultaneously* fluorescence lifetime, three spatial dimensions (through optical sectioning using structured illumination), and wavelength (through multispectral imaging). The importance of spectral separation prior to lifetime imaging has been demonstrated in teeth, where the preferential spectral selection of red-emitting porphyrins, as found in caries, led to a clear demarcation of the carious area in the lifetime map. Although the identification of caries by means of spectral discrimination and longtime gating has already been reported in the literature, our approach additionally enables the co-identification of enamel and dentin. The importance of depth resolution and spectral separation has been demonstrated with fluorescent microspheres, showing two alternative ways of minimizing artefacts caused by out-of-focus light. Where the emission characteristics of different fluorophores allow a total spectral separation, these lifetime artefacts can be completely suppressed without need of optical sectioning. In situations in which this is not possible, optical sectioning is imperative when using a single exponential fit. In addition to the minimization of lifetime artefacts, optical sectioning leads to an enhancement in lateral resolution.

ACKNOWLEDGMENTS

Funding for this research from the U.K. Engineering and Physical Sciences Research Council (EPSRC), the Biotechnology and Biological Sciences Research Council (BBSRC), and the Paul Instrument Fund of the Royal Society is gratefully acknowledged. S.E.D. W. acknowledges an EPSRC studentship. D.S. E. acknowledges an EPSRC CASE studentship with Kentech Instruments Ltd.

REFERENCES

1. J. R. Lakowicz (1999) *Principles of Fluorescence Spectroscopy* (2nd ed.), Plenum Press, New York.
2. M. Straub and S. W. Hell (1998) *Appl. Phys. Lett.* **73**, 1769–1771.
3. M. A. A. Neil, R. Juškaitis, and T. Wilson (1997) *Opt. Lett.* **22**, 1905–1907.
4. J. Siegel, D. S. Elson, S. E. D. Webb, D. Parsons-Karavassilis, S. Lévêque-Fort, M. J. Cole, M. J. Lever, P. M. W. French, M. A. A. Neil, R. Juškaitis, L. O. Sucharov, and T. Wilson (2001) *Opt. Lett.* **26**, 1338–1340.
5. K. C. Benny Lee, J. Siegel, S. E. D. Webb, S. Lévêque-Fort, M. J. Cole, R. Jones, K. Dowling, P. M. W. French, and M. J. Lever (2001) *Biophys. J.* **81**, 1265–1274.
6. Optical Insights, LLC, 1807 Second St, Suite 60, Santa Fe, NM 87505, http://www.optical-insights.com, US Patents: "Multispectral 2D Imaging Spectrometer," U.S. Patent and Trademark Office Serial Nos. 5,926,283 and 5,982,497.
7. R. R. Alfano and S. S. Yao (1981) *J. Dent. Res.* **60**, 120–122.
8. K. Konig, H. Schneckenburger, and R. Hibst (1999) *Cell. Mol. Biol.* **45**, 233–239.
9. U. Hafstrom-Bjorkman, F. Sundstrom, and J. J. ten Bosch (1991) *Acta Odontol. Scand.* **49**, 133–138.
10. M. J. Cole, J. Siegel, S. E. D. Webb, R. Jones, K. Dowling, M. J. Dayel, D. Parsons-Karavassilis, P. M. W. French, M. J. Lever, L. O. D. Sucharov, M. A. A. Neil, R. Juškaitis, and T. Wilson (2001) *J. Microsc.* **203**, 246–257.